THE JOURNAL OF PHYSICAL CHEMISTRY A

Article

Cite This: J. Phys. Chem. A 2018, 122, 3353−3364

pubs.acs.org/JPCA

Effects of the Level of Electronic Structure Theory on the Dynamics of the F^- + CH_3I Reaction

Tibor Győri,[†] Balázs Olasz,[†] Gábor Paragi,[‡] and Gábor Czakó*[,†]

[†]Department of Physical Chemistry and Materials Science, Institute of Chemistry, University of Szeged, Rerrich Béla tér 1, Szeged H-6720, Hungary

[‡]MTA-SZTE Biomimetic Systems Research Group, University of Szeged, Dóm tér 8, Szeged H-6720, Hungary

Supporting Information

ABSTRACT: Accuracy of the different levels of electronic structure theory is frequently studied for stationary-point properties; however, little is known about the effects of the electronic structure methods and basis sets on the dynamics of chemical reactions. Here we report such an investigation for the F^- + CH_3I S_N2 and proton-transfer reactions by developing 20 different analytical potential energy surfaces (PESs) obtained at the HF/DZ, HF/TZ, HF-D3(BJ)/DZ, HF-D3(BJ)/TZ, MP2/DZ, MP2/TZ, MP2-F12/DZ, MP2-F12/TZ, CCSD/DZ, CCSD-F12b/DZ, CCSD(T)/DZ, CCSD(T)-F12b/DZ, OQVCCD(T)/DZ, B97-1/TZ, PBE0/TZ, PBE0-D3(BJ)/TZ, M06-2X/TZ, M06-2X-D3(0)/TZ, B2PLYP/TZ, and B2PLYP-D3(BJ)/TZ levels of theory, where DZ and TZ denote the aug-cc-pVDZ and aug-cc-pVTZ basis sets with a relativistic effective core potential and the corresponding bases for iodine. Millions of quasiclassical trajectories on these PESs reveal that (a) in the case of standard methods, increasing the basis from DZ to TZ decreases the S_N2 cross sections by 20−30%; (b) the explicitly correlated F12 reactivity is converged with a DZ basis; (c) the quasi-variational OQVCCD(T) and the CCSD(T) methods provide virtually the same cross sections; (d) the above DFT functionals give significantly larger S_N2 cross sections than the ab initio methods; (e) retention S_N2 cross sections show striking method and basis dependence and double inversion is substantially enhanced with a TZ basis or F12 methods; (f) the TZ basis doubles the DZ proton-transfer reactivity; (g) at a high collision energy ab initio methods show dominance of backward scattering, in agreement with experiment, whereas most DFT functionals provide slight forward preference; and (h) at high energy the ab initio correlation (DFT) methods slightly underestimate (overestimate) the CH_3F internal energy excitations, whereas the broad experimental distribution is qualitatively reproduced.

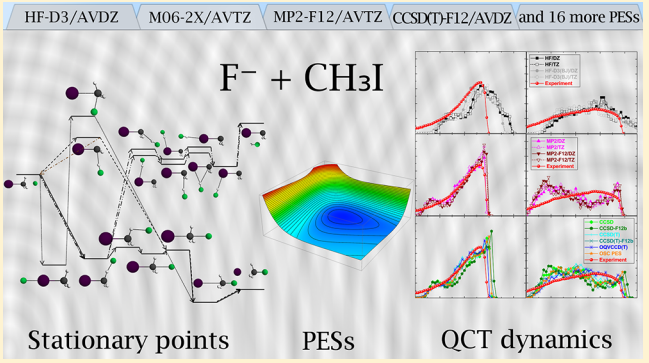

I. INTRODUCTION

Understanding the dynamics and mechanisms of chemical reactions at the deepest atomic and molecular level is one of the main goals of chemistry. Nowadays we can achieve this goal by applying the laws of physics to the chemical systems and utilizing computer resources. Using the Born−Oppenheimer approximation[1] the reaction dynamics simulations have to deal with both the electronic structure and nuclear motion computations. The former provides the potential energy surface (PES), which governs the motion of the nuclei in a chemical reaction. The latter can be performed using either quantum or (quasi)classical methods, where the PES represents the potential energy operator or provides the forces, respectively. Thus in a reaction dynamics simulation the accuracy of the PES usually determines the reliability of the dynamics results. Because the Schrödinger equation of the many-electron systems cannot be solved analytically, one has to use one of the different numerical approximate electronic structure methods to compute the potential energies. The accuracy of the electronic structure methods and basis sets is usually tested for stationary-point properties, that is, barrier heights, reaction enthalpies, dissociation energies, and so on, and little is known about their effects on the dynamics of chemical reactions. In reaction dynamics studies the standard strategy is to first test the performance of the level of electronic structure theory at stationary points, and on the basis of a few relative energies and computational cost the most appropriate method and basis set combinations are chosen for the analytical PES developments or direct dynamics simulations. However, functionals used in density functional theory (DFT) and basis sets are parametrized and optimized for stationary-point properties, and thus electronic structure computations may perform better for barrier heights and reaction enthalpies than for nonstationary configurations and reaction mechanisms that do not follow the minimum energy pathways. Therefore, the investigations of the effects of the choice of the level of

Received: January 23, 2018
Revised: March 13, 2018
Published: March 16, 2018

ACS Publications © 2018 American Chemical Society

DOI: 10.1021/acs.jpca.8b00770
J. Phys. Chem. A 2018, 122, 3353−3364

electronic structure theory on the dynamics of chemical reactions would be highly desired. Here we report such a study by developing 20 analytical PESs for the $F^- + CH_3I$ reaction based on various ab initio and DFT methods as well as different basis sets. Using the new PESs, reaction dynamics simulations are performed, thereby revealing how the level of electronic structure theory affects the dynamics of the $F^- + CH_3I$ S_N2 and proton-transfer reactions.

We focus on the $F^- + CH_3I$ system because several theoretical and experimental investigations have been recently performed for this reaction,[2−12] providing groundbreaking findings on hydrogen-bonded[2−4,6,8] and front-side complex[9] formations as well as leaving-group effect.[13] The crossed-beam experiments provided detailed scattering angle and product internal energy distributions,[3,4] allowing comparison with theoretical simulations.[8] Following the direct dynamics studies of Hase and coworkers,[3,4,7] in 2017 we reported a high-level analytical ab initio PES for the title reaction, denoted as the Olasz−Szabó−Czakó (OSC) PES, and performed detailed dynamical computations.[8] Despite the fact that theory reproduces most of the experimental features, at high collision energies some disagreement is found between the measured and computed distributions. In 2015, Hase and coworkers[5] compared the MP2 and B97-1 direct dynamics simulations and found significant differences in the integral and differential cross sections. On the basis of their study it seems MP2 captures the backside preference of the measured angular distributions better than DFT with the B97-1 functional. However, in a direct dynamics simulation only a few thousands of trajectories can be computed because for each trajectory thousands of gradients have to be determined on-the-fly by an electronic structure program package. Therefore, the statistical uncertainties can be substantial, especially for the differential cross sections, which may obscure the effect of the electronic structure method on the dynamics and compromise the comparison between the measured and computed differential data. Now it is clear that a computationally feasible strategy performs a detailed electronic structure characterization of the stationary points, which requires only a few energy, gradient, and sometimes Hessian computations, and the dynamics simulations utilizing millions or billions of gradients are just performed using only one (or two) selected method and basis set, which is typically DFT or MP2 with a double-ζ-quality basis. The use of higher level correlation methods or larger basis sets is computationally not feasible at present for systems involving several heavy atoms like carbon and halogens. We overcome this challenge by developing analytical PESs using fits of a few tens of thousands of energy points, which can be computed by advanced correlation techniques including variants of the coupled cluster methods and larger basis sets.[14,15] Thus in the present study we report PESs obtained with the following methods using either or both the aug-cc-pVDZ and aug-cc-pVTZ basis sets: HF and HF-D3(BJ), MP2 and MP2-F12, CCSD and CCSD-F12b, CCSD(T) and CCSD(T)-F12b, OQVCCD(T), DFT with B97-1, PBE0, M06-2X, and B2PLYP without and sometimes with dispersion correction.[16−26] These PESs allow an unprecedented investigation of the effects of the different electronic structure methods and basis sets on the cross sections, reaction probabilities, and angular and internal energy distributions of a chemical reaction. The results may provide new insights into the dynamics of the title reaction, help to resolve the disagreement between theory and experiment, and guide future dynamical investigations of similar systems. The wider scope of the present study is to move beyond thinking in stationary points and to extend our predictive knowledge on the accuracy of the different electronic structure methods and basis sets on the dynamics of chemical reactions. In Section II we describe the details of the analytical PES developments and the reaction dynamics computations. The stationary-point properties and the results of the reactive scattering simulations are discussed in Section III. The paper ends with summary and conclusions in Section IV.

II. COMPUTATIONAL DETAILS

II.A. Analytical Potential Energy Surface Developments. We develop 20 new analytical PESs for the $F^- + CH_3I$ reaction using the following levels of electronic structure theory:

(1) HF/aug-cc-pVDZ
(2) HF/aug-cc-pVTZ
(3) HF-D3(BJ)/aug-cc-pVDZ
(4) HF-D3(BJ)/aug-cc-pVTZ
(5) MP2/aug-cc-pVDZ
(6) MP2/aug-cc-pVTZ
(7) MP2-F12/aug-cc-pVDZ
(8) MP2-F12/aug-cc-pVTZ
(9) CCSD/aug-cc-pVDZ
(10) CCSD-F12b/aug-cc-pVDZ
(11) CCSD(T)/aug-cc-pVDZ
(12) CCSD(T)-F12b/aug-cc-pVDZ
(13) OQVCCD(T)/aug-cc-pVDZ
(14) B97-1/aug-cc-pVTZ
(15) PBE0/aug-cc-pVTZ
(16) PBE0-D3(BJ)/aug-cc-pVTZ
(17) M06-2X/aug-cc-pVTZ
(18) M06-2X-D3(0)/aug-cc-pVTZ
(19) B2PLYP/aug-cc-pVTZ
(20) B2PLYP-D3(BJ)/aug-cc-pVTZ

HF, MP2, CCSD, CCSD(T), and OQVCCD(T) denote Hartree−Fock,[16] second-order Møller−Plesset perturbation theory,[17] coupled cluster singles and doubles,[19] CCSD with perturbative triples,[21] and optimized-orbital quasi-variational coupled cluster doubles with perturbative triples[22] methods, respectively. The novel single-reference OQVCCD(T) method[22] is a superior approximation over CCSD(T), providing a better description of the multireference regions of the global PESs than CCSD(T), and thus testing the performance of the OQVCCD(T) method for reaction dynamics computations, where bond breaking and forming processes occur, is highly desired. F12 and F12b refer to the explicitly correlated variants of the correlation methods,[18,20] and D3(BJ) and D3(0) denote additive dispersion corrections.[27,28] For the DFT computations the B97-1,[23] PBE0,[24] M06-2X,[25] and B2PLYP[26] functionals are selected because B97-1 was shown in the literature to describe the stationary-point properties of the title reaction reasonably well and this functional was used in previous direct dynamics studies,[3−5,7] PBE0 is a popular nonempirical functional that can be contrasted with the widely used M06-2X functional involving many empirical parameters and dispersion correction, while B2PLYP is a double-hybrid functional utilizing HF exchange and MP2 correlation energies, thus usually outperforming the simple hybrid functionals. All of the electronic structure computations employ the correlation-consistent polarized valence double- and triple-ζ basis sets of Dunning[29]

DOI: 10.1021/acs.jpca.8b00770
J. Phys. Chem. A 2018, 122, 3353−3364

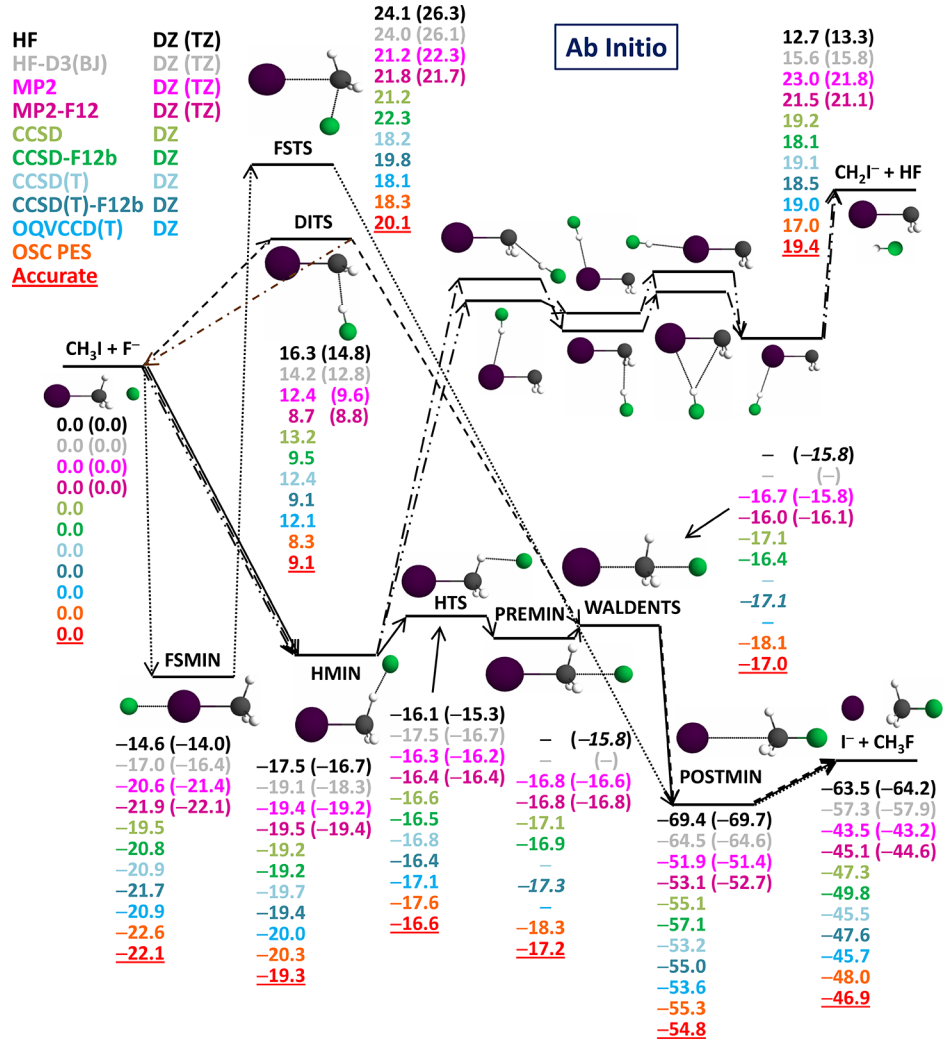

Figure 1. Potential energy surface of the F^- + CH_3I reaction showing the classical relative energies (kcal/mol) of the stationary points corresponding to different ab-initio-based analytical PESs obtained with various methods and the aug-cc-pVDZ (DZ) and aug-cc-pVTZ (TZ) basis sets. The OSC PES and the accurate all-electron CCSD(T)-F12b/QZ-quality benchmark results are taken from ref 8. For PREMIN and WALDENTS some ab initio levels do not provide reasonable stationary points, and the italic numbers can only be obtained with Molpro.

augmented with diffuse functions, denoted as aug-cc-pVDZ (DZ) and aug-cc-pVTZ (TZ). For iodine a relativistic effective core potential replacing the $1s^22s^22p^63s^23p^63d^{10}$ inner core electrons and the corresponding pseudopotential basis sets,[30] aug-cc-pVDZ-PP and aug-cc-pVTZ-PP, are used. All electronic structure computations are performed using the Molpro package,[31] except that the additive dispersion corrections are obtained with the DFT-D3 program.[27,28]

The geometries are taken from ref 8, where the OSC PES was developed based on CCSD(T)-F12b/aug-cc-pVTZ plus core correlation correction, which is obtained from the difference of all-electron and frozen-core energies computed at the CCSD(T)/aug-cc-pCVDZ level of theory. Potential energies are computed at the nuclear configurations of ref 8 with the above-defined 20 different levels of electronic structure theory resulting in roughly 50 000 data points for each PES with small variances in the number of points due to occasional HF and other convergence problems at certain geometries that are discarded. The PESs are represented using the following functional form[32,33]

$$V = \sum_{\mathbf{n}=\mathbf{0}}^{\mathbf{N}} C_{\mathbf{n}} S(y_{12}^{n_{12}} y_{13}^{n_{13}} y_{14}^{n_{14}} \ldots y_{23}^{n_{23}} y_{24}^{n_{24}} \ldots) \quad (1)$$

where y_{ij} denotes Morse-type variables, $\exp(-r_{ij}/a)$, of r_{ij} interatomic distances, a is fixed at 3 bohr, S is a symmetrization operator, $\mathbf{n}$ and $\mathbf{N}$ are collective indices of (n_{12}, n_{13}, n_{14}, ..., n_{23}, n_{24}, ...), and $C_{\mathbf{n}}$ denotes the coefficients that are determined by a weighted linear least-squares fit to the energy points. S generates a symmetrized fitting basis,[32,33] which is explicitly invariant under the permutation of the identical H atoms. The efficient fitting code employed in the present study uses the sophisticated permutationally invariant polynomial theory to obtain the fitting basis, as described in detail in ref 32. Here, for simplicity, the more straightforward eq 1 is used for the discussion, which gives the same PES with a different algorithm. During the fitting, the sum of the exponents in eq 1 is constrained to be ≤ 5, resulting in 3313 coefficients for the H_3CFI^- system. For each energy a weight of $E_0/(E + E_0)$ is used, where E is the energy relative to the global minimum and E_0 is 63 kcal/mol, thereby reducing the root-mean-square errors usually <1 kcal/mol for the chemically important regions of the PESs.

DOI: 10.1021/acs.jpca.8b00770
J. Phys. Chem. A 2018, 122, 3353−3364

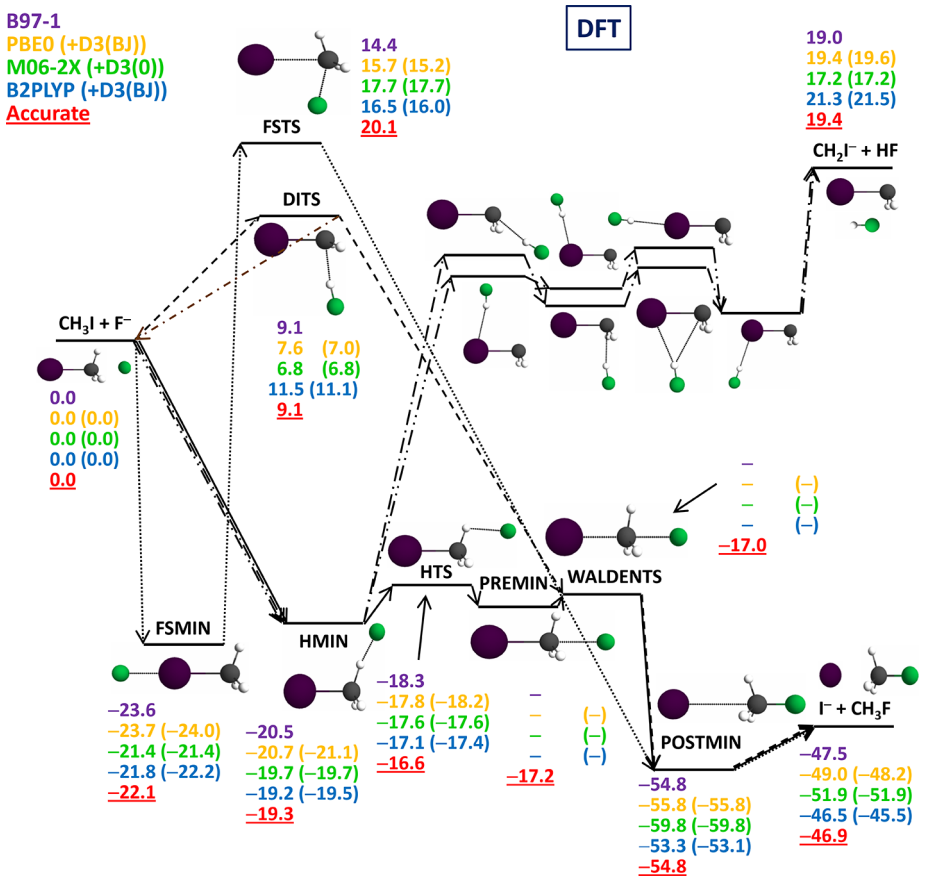

Figure 2. Potential energy surface of the F^- + CH_3I reaction showing the classical relative energies (kcal/mol) of the stationary points corresponding to different DFT-based analytical PESs obtained with various functionals and the aug-cc-pVTZ basis set. The accurate all-electron CCSD(T)-F12b/QZ-quality benchmark results are taken from ref 8. For PREMIN and WALDENTS the present DFT functionals do not provide reasonable stationary points.

II.B. Reaction Dynamics Simulations. Quasiclassical trajectory (QCT) computations are performed for the F^- + $CH_3I(v = 0)$ reaction using the 20 different analytical PESs described above. The quasiclassical ground vibrational state of CH_3I is prepared by standard normal mode sampling,[34] and adjustments to the velocities are done to set the rotational angular momentum to zero. The initial orientation of the reactants is randomly sampled, and the initial distance is set to $(x^2 + b^2)^{1/2}$, where b is the impact parameter and $x = 20$ bohr. Trajectories are run at collision energies (E_{coll}) of 7.4, 15.9, and 35.3 kcal/mol, because at these E_{coll} experimental data are available.[4] b is scanned from 0 to b_{max} with a step of 0.5 bohr. The b_{max} values are around 17, 14, and 11 bohr at the above E_{coll}, respectively, with small variance with the level of electronic structure theory. At each b 5000 trajectories are run, which means 115 000−175 000 trajectories at each E_{coll} and close to a half million trajectories for each PES. Thus the present study considers nearly 10 million trajectories for the 20 PESs. The trajectories are integrated using a time step of 0.0726 fs (3 atomic time units), and each trajectory is propagated until the largest interatomic separation becomes 1 bohr larger than the initial one. Cross sections are obtained by a b-weighted numerical integration of the reaction probabilities over impact parameters.

III. RESULTS AND DISCUSSION

III.A. Electronic Structure Effects on Stationary-Point Properties. Schematic PESs of the F^- + CH_3I reaction showing the relative energies of the stationary points obtained by optimizations on the various ab initio and DFT PESs are shown in Figures 1 and 2, respectively. (Note that even if HF-D3(BJ) contains empirical dispersion correction, it is listed among the ab initio methods for comparison.) The relative energies corresponding to the PESs obtained at different levels of electronic structure theory are compared to the accurate all-electron CCSD(T)-F12b/QZ-quality benchmark values.[8] The S_N2 channel can proceed via the Walden-inversion pathway involving a hydrogen-bonded complex (HMIN, C_s), a hydrogen-bonded transition state (HTS, C_s), a prereaction ion-dipole complex (PREMIN, C_{3v}), a Walden-inversion transition state (WALDENTS, C_{3v}), and a postreaction ion-dipole complex (POSTMIN, C_{3v}), leading to the I^- + CH_3F products. Besides the Walden-inversion mechanism, the S_N2 reaction can occur via the double-inversion and the front-side attack retention pathways.[35,8] As our previous reaction dynamics simulations showed,[8,35] the first step of double inversion is a proton-abstraction-induced inversion via a so-called double-inversion transition state (DITS, C_s), followed by a substitution event via Walden inversion. As recent studies pointed out, the above-described double-inversion pathway does not correspond to an intrinsic reaction coordinate path.[7,10] The front-side attack proceeds via a high-energy transition state (FSTS, C_s), with F−

DOI: 10.1021/acs.jpca.8b00770
J. Phys. Chem. A 2018, 122, 3353−3364

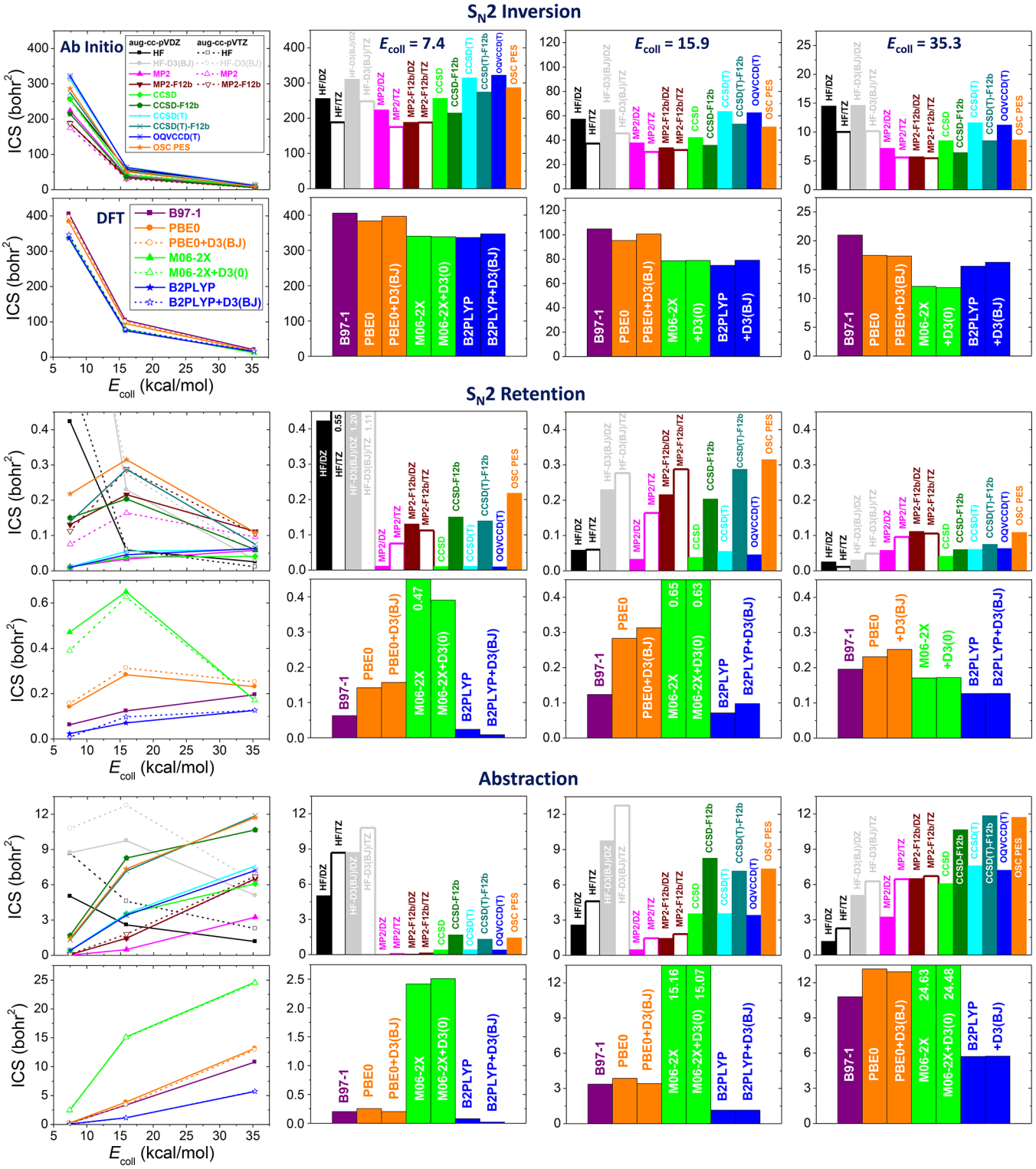

Figure 3. Cross sections for the F^- + CH_3I S_N2 and proton-abstraction reactions obtained on various ab-initio- and DFT-based PESs at different collision energies.

C−I angle of ∼80°.[8] In the entrance channel of the title reaction a halogen-bonded front-side complex (FSMIN, C_{3v}) can also be formed, which was recently shown to play a significant role in the dynamics.[9] Among the other possible product channels of the F^- + CH_3I reaction the most important one is the proton-abstraction (proton-transfer) channel leading to HF + CH_2I^-. There are several minima and transition states involved in the endothermic proton-abstraction process, as indicated in Figures 1 and 2; here we just focus on the energy of the product asymptote.

Before we discuss the accuracy of the different levels of electronic structure theory, we note that the F^- + CH_3I S_N2 reaction is quite unique, because the existence of the traditional PREMIN and WALDENTS depends very sensitively on the

DOI: 10.1021/acs.jpca.8b00770
J. Phys. Chem. A 2018, 122, 3353−3364

electronic structure methods, as seen in Figures 1 and 2. DFT computations with the present and several other (see ref 2) functionals do not find these stationary points. Although some ab initio methods can determine PREMIN and WALDENTS with only a 0.2 kcal/mol energy difference, the S_N2 channel of the $F^- + CH_3I$ reaction can be viewed as HMIN → HTS → POSTMIN → products, as seen in the literature.[2,12]

As shown in Figure 1 the HF method performs very poorly for most of the stationary-point energies. It overestimates the S_N2 exothermicity by ∼17 kcal/mol (∼40% relative error), underestimates the endothermicity of the proton-transfer channel by ∼6 kcal/mol (∼30%), and substantially overestimates the energies of the DITS and FSTS. Dispersion correction significantly improves the HF results; for example, 1/3 of the errors disappear, but most of the results are still unreasonable. MP2 and MP2-F12 methods provide chemically accurate (error <1 kcal/mol) relative energies for many stationary points such as FSTS, HMIN, HTS, PREMIN, WALDENTS, and DITS, but underestimate the S_N2 exothermicity by 2−4 kcal/mol, depending on the basis set, and overestimate the proton-abstraction endothermicity by ∼2 kcal/mol. In some cases the basis set effects can also be significant because the MP2 DZ and TZ energies can differ by 1 to 2 kcal/mol. The largest basis set effect of 2.8 kcal/mol is found for the DITS. As expected, the MP2-F12 method shows much faster basis convergence and in some cases provides MP2/TZ quality results with the DZ basis (see, for example, DITS or HF + CH_2I^-). CCSD and CCSD-F12b methods do not always improve the corresponding MP2 results. For example, whereas MP2 underestimates the S_N2 exothermicity, CCSD-F12b overestimates it by ∼3 kcal/mol. The CCSD(T) method can definitely provide chemical accuracy, although where the basis set effects are significant one needs to employ CCSD(T)-F12b if a DZ basis is used (see DITS). The CCSD(T) and OQVCCD(T) methods provide the same relative energies within 0.1 to 0.4 kcal/mol for all the stationary points, showing that the use of single-reference methods is adequate for these geometries. The all-electron CCSD(T)-F12b/TZ-quality OSC PES (ref 8) and the CCSD(T)-F12b/DZ PES are expected to give similar results because the basis set effect, in the case of F12 computations, is 0.1 to 0.4 kcal/mol and the core correlation corrections are 0.1 to 0.8 kcal/mol. For most of the stationary points, the two PESs agree within the expected uncertainty. The fact that for the stationary points shown in Figure 1 the CCSD(T)-F12b/DZ PES agrees better with the benchmark data than the higher level OSC PES can be due to favorable error cancelation during the fitting of the former PES or the different treatment of the fragment data. For the OSC PES energies of the reactant and product channels are obtained assuming additivity of the fragment energies, whereas in the present study the fragment data are obtained with supermolecule computations. Of course, we still do not know how the better agreement with the benchmark stationary-point data shows up in the reaction dynamics results (see Section III.B).

The DFT computations using the four different functionals of the present study clearly improve the HF results and in some cases provide chemical accuracy, as shown in Figure 2. The B97-1 functional, which was used in previous direct dynamics studies,[3−5,7] gives excellent agreement with the benchmark data for all stationary points, except for the FSTS, where B97-1 seriously underestimates the barrier height by ∼6 kcal/mol. Nevertheless, the reaction exothermicity (S_N2) and endothermicity (proton transfer) are reproduced well within 1 kcal/mol. PBE0 gives a slightly better front-side attack barrier height (although still with an error of 4 to 5 kcal/mol) and excellent proton-transfer endothermicity but overestimates the S_N2 exothermicity by ∼2 kcal/mol, an error that can be reduced by 0.8 kcal/mol by applying dispersion correction. M06-2X performs with chemical accuracy for FSMIN, HMIN, and HTS and gives the best front-side attack barrier height among the four functionals but performs the worst for the exo- and endothermicities, overestimating by 5 kcal/mol and underestimating by 2 kcal/mol, respectively. Here the D3(0) dispersion correction has effects <0.1 kcal/mol, as expected, because M06-2X contains dispersion correction by design. The double-hybrid B2PLYP functional overall gives good results, except it overestimates the proton-transfer endothermicity by 2 kcal/mol. Dispersion corrections can be in the range of 0.2 to 1.0 kcal/mol, but they usually do not improve the agreement with the benchmark energies. We can conclude that some of the DFT functionals can compete with MP2, but for definitive results for all of the stationary points the CCSD(T) method is needed. Does the above statement hold for the dynamics as well?

III.B. Electronic Structure Effects on Reaction Dynamics. Cross sections for the different channels of the $F^- + CH_3I$ reaction corresponding to the various ab-initio- and DFT-based PESs are shown in Figure 3. The S_N2 inversion cross sections are large and decrease with increasing E_{coll}, as expected in the case of an exothermic reaction with submerged barrier. This qualitative behavior is obtained by all of the electronic structure levels; however, significant quantitative differences exist in the cross section data. At all three E_{coll}, MP2 decreases the HF cross sections, whereas CCSD increases and CCSD(T) further increases the MP2 results. For example, at E_{coll} = 35.3 kcal/mol the HF, MP2, CCSD, and CCSD(T) cross sections are 14.5, 7.2, 8.5, and 11.6 bohr^2, respectively, using the aug-cc-pVDZ basis. Note that the MP2 result is in good agreement with a previous MP2/DZ direct dynamics cross section of 6.4 ± 1.1 bohr^2.[5] The OQVCCD(T) and CCSD(T) methods give virtually the same cross sections, indicating that most of the configurations used in the PES developments do not have serious multireference character. The dispersion correction slightly increases the HF cross sections, but this effect diminishes at higher E_{coll}. Increasing the basis from DZ to TZ the cross sections substantially drop by ∼30% at the HF level, and a similar trend, albeit less significant (∼20%), is seen at the MP2 level of theory. MP2-F12 gives MP2/TZ-quality cross sections with a DZ basis. Furthermore, because of fast basis set convergence of the F12 methods, MP2-F12 provides almost the same results with DZ and TZ bases. In accord with the MP2 results, the CCSD-F12b and CCSD(T)-F12b cross sections are ∼20% below the corresponding standard results. On the basis of the MP2-F12 results, the CCSD(T)-F12b/DZ cross section is expected to be basis-set-converged, which is supported by the fact that the CCSD(T)-F12b/TZ-quality OSC PES (ref 8) gives virtually the same cross sections as CCSD(T)-F12b/DZ does, even if some differences exist in the stationary-point energies. Overall DFT provides significantly larger S_N2 inversion cross sections than the ab initio methods. At E_{coll} = 7.4, 15.9, and 35.3 kcal/mol the high-level OSC PES gives cross sections of 287, 51, and 9 bohr^2, respectively, whereas the corresponding DFT results are 330−410, 74−105, and 11−22 bohr^2 depending on the functional. B97-1 provides the largest cross sections of 406, 105, and 21 bohr^2, respectively

DOI: 10.1021/acs.jpca.8b00770
J. Phys. Chem. A 2018, 122, 3353−3364

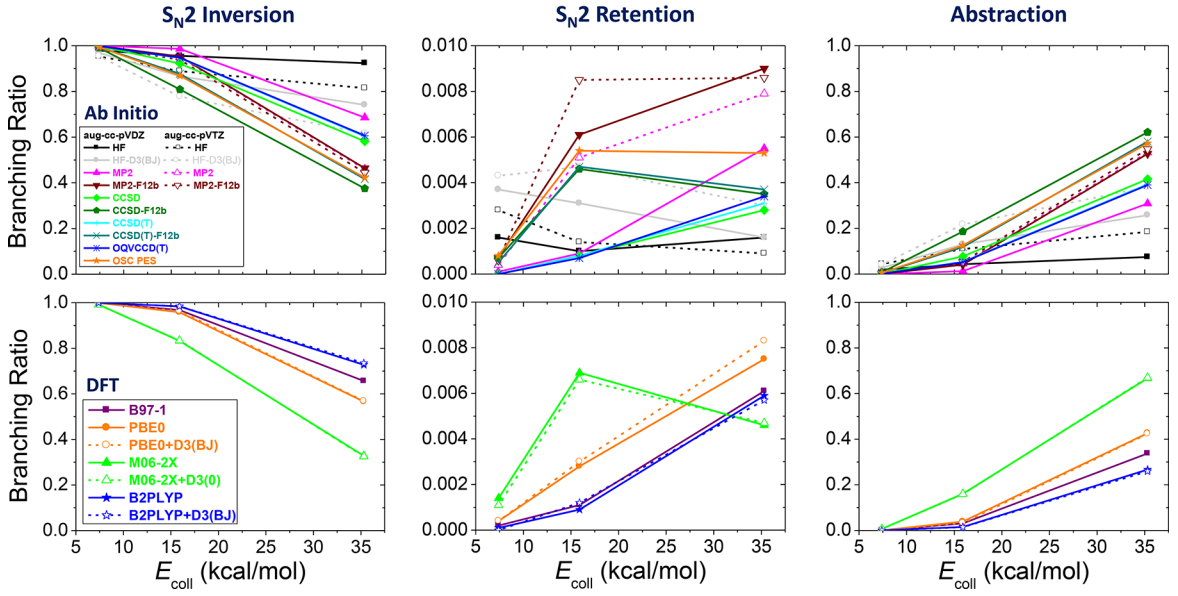

Figure 4. Branching ratios of the I^- + CH_3F(inversion), I^- + CH_3F(retention), and HF + CH_2I^- product channels of the F^- + CH_3I reaction obtained on various ab-initio- and DFT-based PESs at different collision energies.

and the lowest (best) ones are obtained with the M06-2X and B2PLYP functionals. The fact that B97-1 overestimates the cross sections is in accord with the previous findings of Hase and coworkers[5] who obtained a B97-1/DZ cross section of 31 ± 8 bohr^2 at E_{coll} = 35.3 kcal/mol, which is in good agreement with our value of 21 bohr^2 obtained with a larger TZ basis, which may decrease the cross sections. At high E_{coll}, clearly M06-2X provides the best agreement with the accurate OSC PES value, that is, 12 versus 9 bohr^2. Dispersion corrections usually slightly increase the PBE0 and B2PLYP cross sections and have negligible effects on the M06-2X results, the functional of which already includes dispersion effects.

Figure 3 also shows the cross sections for the S$_N$2 retention pathways (double inversion and front-side attack). Here the method dependence is more significant than in the case of the inversion channel. At E_{coll} = 7.4 kcal/mol, HF, especially with dispersion correction, gives an order of magnitude larger retention cross sections than the correlation methods. At higher E_{coll}, the HF/DZ cross sections are similar to the other DZ results. As seen in Figure 3, the basis set effects on the retention cross sections are striking, especially at low E_{coll}. For example, at E_{coll} = 7.4 kcal/mol the MP2/TZ result is 6.5 times larger than the MP2/DZ value. Furthermore, CCSD-F12b and CCSD(T)-F12b provide 15 and 13 times larger cross sections than CCSD and CCSD(T), respectively. At the HF level the basis set dependence is modest, indicating that the basis set effect on the correlation energy increases the retention cross sections. The OSC PES provides substantial retention reactivity, similar to the CCSD(T)-F12b/DZ results. At the highest E_{coll} of 35.3 kcal/mol the basis set effect is less significant (20−60%) than at the lower collision energies. This may be explained by the fact that at lower collision energies the dominant retention mechanism is double inversion, whereas at higher E_{coll} retention mainly proceeds via the front-side attack pathway. The basis set effects on the double-inversion barrier height are in accord with the above findings because the standard methods with DZ basis give barriers ∼3 kcal/mol larger than the F12 methods or TZ basis. The DFT results show significant functional dependence on the retention cross sections. B2PLYP provides the smallest cross sections, and B97-1 and PBE0 give larger and larger retention reactivities. At the lowest two collision energies M06-2X gives the largest cross sections, about two times the PBE0 results, whereas at E_{coll} = 35.3 kcal/mol the M06-2X cross section is below that of PBE0 and B97-1. Most of these findings are also in accord with the double-inversion barrier heights of 6.8, 7.6, 9.1, and 11.5 kcal/mol for M06-2X, PBE0, B97-1, and B2PLYP, respectively. However, it is important to note that even if the double-inversion barriers corresponding to B97-1 and CCSD(T)-F12b/DZ are the same, the latter gives about twice as large retention cross sections than the former. Thus the accuracy of the dynamics cannot be simply predicted based on stationary-point properties. Furthermore, it is also worth emphasizing that one needs either a TZ basis or an explicitly correlated method to obtain significant double-inversion reactivity. Our DFT computations utilize a TZ basis, and thus the above functionals may give smaller double-inversion probabilities with a DZ basis. This finding is important because all of the previous direct dynamics studies of the title reaction employed a DZ basis set, which may diminish the double-inversion channel.

For the abstraction (proton transfer) channel the different methods give qualitatively different excitation functions, as shown in Figure 3. At the HF level the cross sections decrease with increasing E_{coll}, whereas the ab initio correlation methods and DFT provide increasing cross sections as E_{coll} increases. The accurate adiabatic, zero-point-energy (ZPE)-corrected enthalpy of the F^- + CH_3I → HF + CH_2I^- reaction is 15.9 kcal/mol, and thus at the lowest E_{coll} of the present study, 7.4 kcal/mol, this channel is energetically not available. However, nonzero abstraction reactivity can be obtained at E_{coll} = 7.4 kcal/mol due to two reasons: (1) The PES may underestimate the endothermicity or (2) QCT can produce products with internal energies less than the corresponding ZPEs.[36] The HF method gives much larger cross sections at E_{coll} = 7.4 kcal/mol than the other methods, in accord with the fact that HF underestimates the endothermicity by 6 to 7 kcal/mol. However, dispersion correction further increases the HF cross sections even if the endothermicity increases as well. This

DOI: 10.1021/acs.jpca.8b00770
J. Phys. Chem. A 2018, 122, 3353−3364

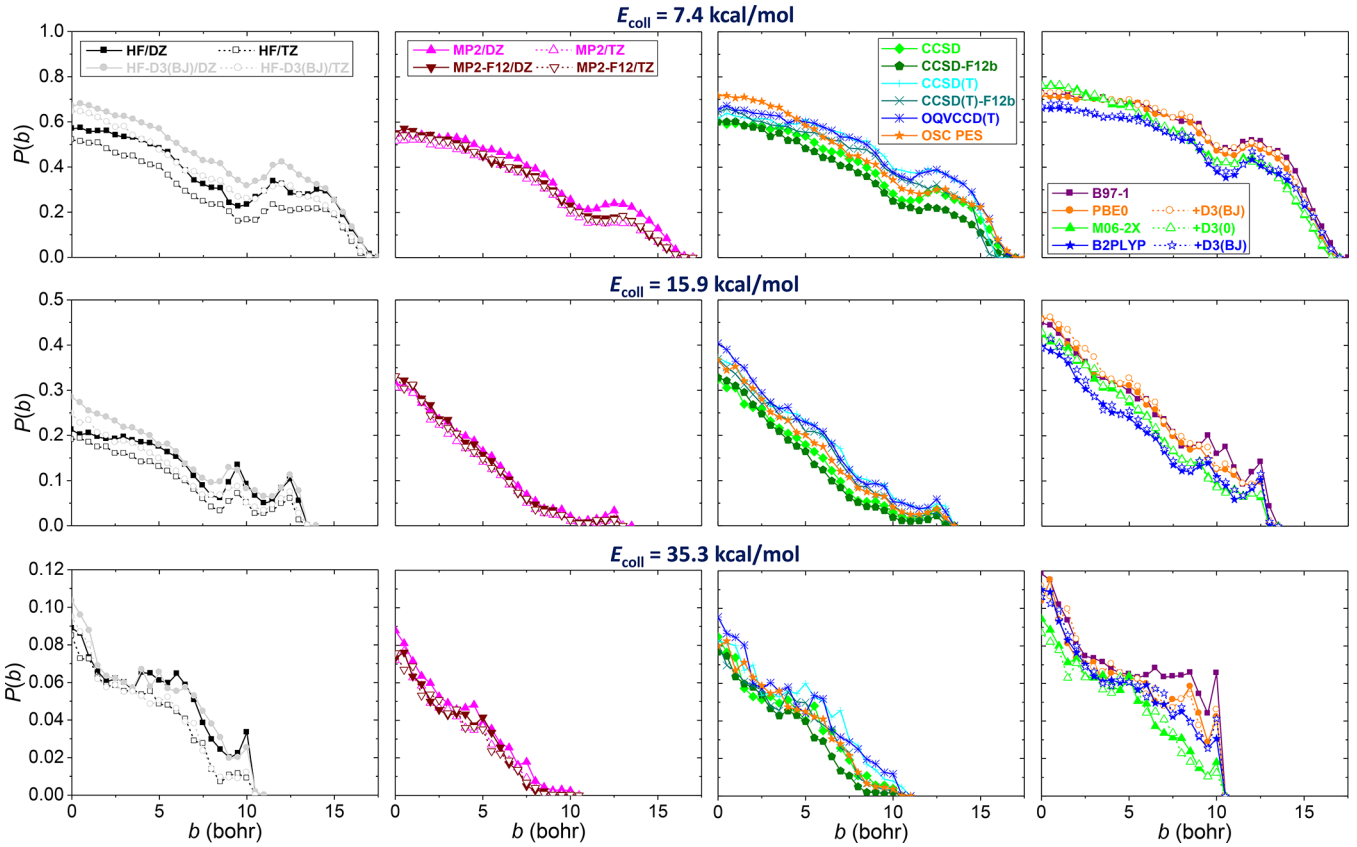

Figure 5. Reaction probabilities as a function of impact parameters for the F^- + CH_3I S_N2 reaction obtained on various ab-initio- and DFT-based PESs at different collision energies.

finding is also true for the higher collision energies, where the abstraction channel is not unphysical. Thus this is another example where the dynamics cannot be predicted based simply on the stationary-point properties. The other ab initio methods give small cross sections at E_{coll} = 7.4 kcal/mol. The smallest cross sections are obtained with the MP2 methods, which overestimate the endothermicity by 2−4 kcal/mol, as seen in Figure 1. The B97-1, PBE0, and B2PLYP functionals give small cross sections at the lowest E_{coll}, whereas M06-2X results in an order of magnitude larger reactivity. This is accord with the fact that M06-2X gives the lowest endothermicity among the DFT functionals, ∼2 kcal/mol below the accurate value. As E_{coll} increases the cross sections increase as well, and their relative magnitude reflects the order of the endothermicities; that is, the cross sections decrease as the endothermicities increase using M06-2X, PBE0, B97-1, and B2PLYP, in order. At the B97-1/DZ level a recent direct dynamics study reported a proton-transfer cross section of 7.5 ± 2.9 $bohr^2$ at E_{coll} = 35.3 kcal/mol, in reasonable agreement with our B97-1/TZ result of 10.8 $bohr^2$. In the case of the ab initio levels of theory the method dependence of the cross sections depends on the collision energy. Whereas HF seriously overestimates the abstraction reactivity at low E_{coll}, at 15.9 kcal/mol the HF results are comparable to the other cross sections and at E_{coll} = 35.3 kcal/mol the HF method provides the smallest cross sections. Again, it worth emphasizing that this E_{coll} dependence of the reactivity cannot be predicted based on the method dependence of the endothermicity. As Figure 3 shows, the proton-transfer probability significantly depends on the basis set as MP2 provides roughly twice as large reactivity with a TZ basis compared with the DZ result. The MP2/TZ abstraction cross sections agree very well with the MP2-F12 DZ and TZ results, showing the good basis set convergence of the F12 methods. The MP2 basis set effects are in accord with the coupled cluster results, as CCSD-F12b and CCSD(T)-F12b give almost twice as larger cross sections as the standard CCSD and CCSD(T) methods. Similar to the case of the S_N2 reactivity, CCSD(T) and OQVCCD(T) give similar cross sections. Furthermore, CCSD(T)-F12b/DZ and the CCSD(T)-F12b/TZ-quality OSC PES provide virtually the same proton-transfer reactivity, showing again that the dynamics is basis set converged with a DZ basis if F12 correlation methods are used.

The branching ratios of the above-discussed different product channels are shown in Figure 4. At the lowest E_{coll} most of the electronic structure levels provide >99% probability for the S_N2 channel, except the Hartree−Fock levels that produce 2−4% HF + CH_2I^- beside the 96−98% I^- + CH_3F. As previously mentioned, the nonzero proton-transfer probability at E_{coll} = 7.4 kcal/mol is unphysical, caused by ZPE leaking. As E_{coll} increases, the abstraction product ratio increases at the expense of the S_N2 channel. The HF + CH_2I^- product ratios vary between 1 and 22% at E_{coll} = 15.9 kcal/mol and between 7 and 67% at E_{coll} = 35.3 kcal/mol depending on the level of electronic structure theory. Whereas the HF method gives unphysically large proton-transfer ratio at the lowest E_{coll}, this ratio just slightly increases with E_{coll}, resulting in only 7% HF + CH_2I^- at E_{coll} = 35.3 kcal/mol with a DZ basis. Enlarging the basis size or adding dispersion correction increases the Hartree−Fock abstraction ratio up to 38%. At E_{coll} = 35.3 kcal/mol MP2 provides 31% proton-transfer ratio with a DZ basis, the ratio of which increases to 52−55% if a TZ basis or MP2-F12 is used. At the same E_{coll}, CCSD, CCSD(T), and

DOI: 10.1021/acs.jpca.8b00770
J. Phys. Chem. A 2018, 122, 3353−3364

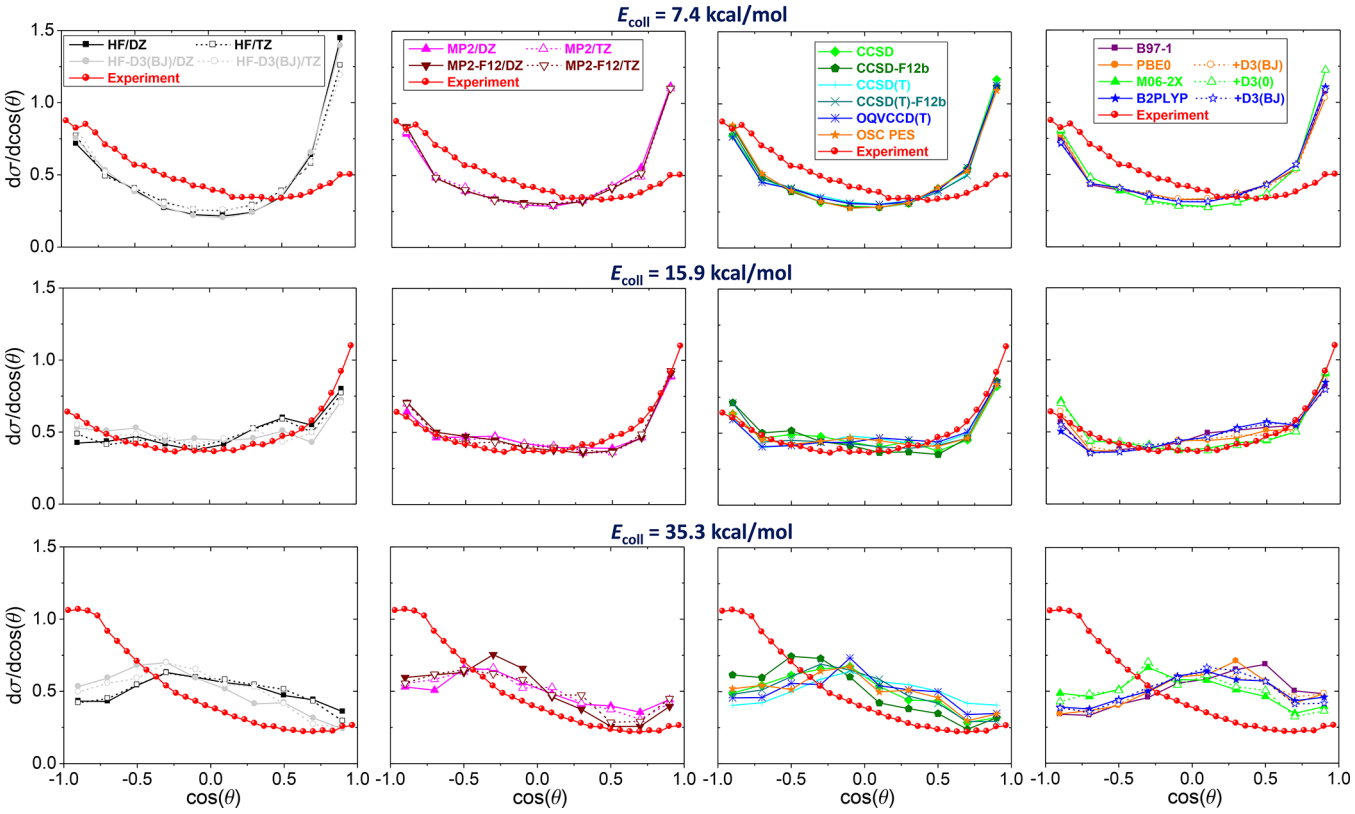

Figure 6. Normalized scattering angle distributions for the F^- + CH_3I S_N2 reaction obtained on various ab-initio- and DFT-based PESs at different collision energies. The experimental data are taken from ref 4.

OQVCCD(T) provide ~40% HF + CH_2I^-, whereas CCSD-F12b, CCSD(T)-F12b, and the OSC PES give ratios around 60%. Thus it seems that the basis set effect on the S_N2 versus proton-transfer ratio is significant because the use of a TZ basis or F12 methods, which provide TZ-quality results with a DZ basis, substantially increases the abstraction ratio. The different DFT functions with a TZ basis give 30−40% abstraction ratio at E_{coll} = 35.3 kcal/mol, except M06-2X, which overestimates the proton-transfer probability, providing 67% HF + CH_2I^-. The S_N2 retention channel is minor, with <1% ratio varying significantly with the level of electronic structure theory. Similar to the abstraction channel, the basis set effects are the most notable because significantly larger retention fractions can be obtained with a TZ basis or an F12 method relative to standard DZ results. As Figure 4 shows, B97-1, PBE0, and B2PLYP provide retention ratios increasing with E_{coll}, whereas M06-2X gives different E_{coll} dependence, in agreement with the F12 ab initio results.

Opacity functions (reaction probabilities as a function of b) for the S_N2 channel obtained with the different ab initio and DFT PESs are shown in Figure 5. Reaction probabilities usually decrease with increasing b and vanish at around 17, 14, and 11 bohr at E_{coll} of 7.4, 15.9, and 35.3 kcal/mol, respectively. The DFT S_N2 reaction probabilities are somewhat larger than the ab initio ones, in accord with the larger DFT cross sections. The most important difference between the shapes of the opacity functions is seen at the highest E_{coll}, where the ab initio correlation methods show almost linearly decreasing reaction probabilities between 0 and 11 bohr, whereas the DFT methods, especially in the case of B97-1, show significant reactivity at the large b values between 5 and 11 bohr and the reaction probability steeply drops at b_{max}. This indicates different scattering dynamics at high E_{coll} depending on the electronic structure level of theory, which will be further discussed below.

Scattering angle distributions for the F^- + CH_3I S_N2 reaction corresponding to the different electronic structure levels of theory are presented in Figure 6. Here the various theoretical results can be directly compared to experiment (ref 4), thereby testing the effects of the electronic structure methods and basis sets on the reaction dynamics. At E_{coll} = 7.4 kcal/mol the different ab initio levels and DFT functionals provide qualitatively similar, nearly isotropic angular distributions with backward−forward dominance and slight preference toward forward scattering. The experimental angular distribution is also similar but rather backward scattered. At E_{coll} = 15.9 kcal/mol the measured angular distribution is also nearly isotropic with slight forward scattering dominance, which is excellently reproduced by theory. Here significant differences are not seen between the various computed distributions. This finding is important in light of the fact that DFT provides about twice as large integral cross sections as the ab initio levels. At the highest E_{coll} of 35.3 kcal/mol, qualitative difference is found between the ab initio and DFT angular distributions. The ab initio levels provide slightly backward-scattered distributions, in agreement with experiment, whereas all of the DFT functionals, except M06-2X, show slight preference toward forward directions, in accord with the shape of the opacity functions discussed above. Thus it seems that at high E_{coll} most of the DFT functionals cannot reproduce experiment, probably due to the fact that these functionals are optimized to minimum-energy pathways. Hase and coworkers[5] also found that MP2 may capture the high-E_{coll} dynamics better than DFT, although their direct dynamics study did not have enough statistics to

DOI: 10.1021/acs.jpca.8b00770
J. Phys. Chem. A 2018, 122, 3353−3364

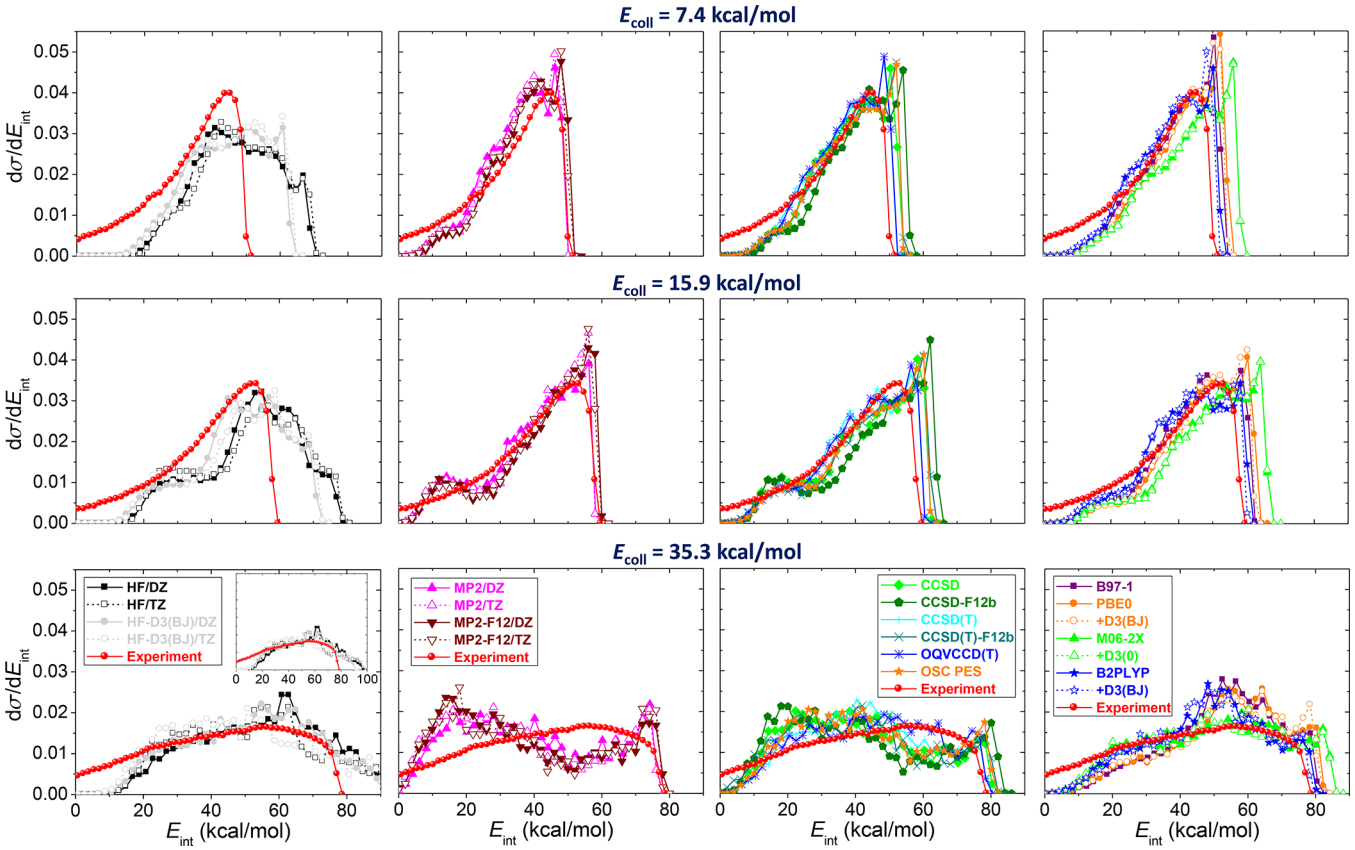

Figure 7. Normalized product internal energy distributions for the F^- + CH_3I S_N2 reaction obtained on various ab-initio- and DFT-based PESs at different collision energies. The experimental data are taken from ref 4.

draw a definitive conclusion from the scattering angle distributions. In the present study we clearly see that MP2 reproduces experiment better than DFT, especially with B97-1. However, we have to note that experiment shows more backward scattering than MP2 and neither the higher level correlation methods, that is, CCSD, CCSD(T), and OQVCCD(T), nor the larger basis sets can qualitatively change the angular distributions and can improve the agreement with experiment. Thus if we do not assume a large experimental uncertainty, then two sources of errors can be the reason for the theoretical−experimental discrepancy: (1) Quantum effects may be significant, which cannot be described by QCT, or (2) the sampling of the configurations used for the analytical PES developments may need to be improved. Of course, (1) is not expected at high E_{coll} and (2) is unlikely because our analytical PES-based results agree well with the fitting-error-free direct dynamics where comparison is possible.

Internal energy distributions for the CH_3F product of the F^- + CH_3I S_N2 reaction are shown in Figure 7, where experimental data are also available. The computed internal energies are obtained as $K + V - E_{ZPE}$, where K is the kinetic energy of CH_3F at the center of mass frame, V is the potential energy of the CH_3F product relative to the equilibrium value, and E_{ZPE} is the harmonic zero-point energy of CH_3F corresponding to the given PES. At the lowest collision energies of 7.4 and 15.9 kcal/mol, the crossed-beam experiment[4] shows hot distributions peaking at the largest available internal energies, indicating the dominance of indirect mechanisms, in accord with the nearly isotropic scattering angle distributions. The experimental data are very well reproduced by the various ab initio correlation methods and DFT functionals. Perhaps M06-2X performs the worst, producing too much internal excitation, because this functional seriously overestimates the exothermicity (by 6 kcal/mol), which leaves more available energy for the products. The HF method gives unreasonable internal energy distributions shifting by ∼20 kcal/mol toward higher energies. It is also somewhat expected because HF overestimates the S_N2 exothermicity by ∼17 kcal/mol. Furthermore, the shape of the distributions is also not well reproduced by the HF method, as seen in Figure 7. The dispersion correction slightly improves the HF results, but the distributions are still not reliable. At the highest E_{coll} of 35.3 kcal/mol the internal energy distribution qualitatively changes, becoming much broader than at lower E_{coll}. Theory can qualitatively reproduce experiment, but the agreement between the measured and computed distributions is not as good as at the lower E_{coll}. HF now captures the shape of the distribution, but the HF data are still shifted by ∼20 kcal/mol toward hotter internal energies; thus the HF method is not adequate to describe the product energy partitioning. The various ab initio correlation methods provide similar distributions, although subtle differences exist. For example, it seems that the OQVCCD(T) method gives slightly better, actually very good, agreement with experiment than the other methods. All ab initio correlation methods provide slightly larger populations at low internal energies and underestimate the high internal energy region. In contrast, B97-1, PBE0, and B2PLYP overestimate the high internal energy populations. M06-2X gives quite good agreement with experiment, except that the distribution is shifted by ∼6 kcal/mol toward higher internal energies. Even if differences exist and further

DOI: 10.1021/acs.jpca.8b00770
J. Phys. Chem. A 2018, 122, 3353−3364

improvement of theory is desired, both the ab initio and the DFT methods provide qualitative agreement with the measured broad internal energy distribution at high collision energy.

IV. SUMMARY AND CONCLUSIONS

It is well known and has been frequently studied that the stationary-point properties such as barrier heights, reaction enthalpies and so on, as well as minimum energy pathways of chemical systems may depend on the electronic structure methods and basis sets. However, little is known about the effects of the level of the electronic structure theory on the dynamics of chemical reactions. To study these dynamical effects the knowledge of the global PES is needed, whose computation is much more demanding than the determination of a few stationary-point properties. Our analytical PES-based approach allows the development of PESs at many different levels of electronic structure theory, thereby allowing efficient dynamical simulations, revealing the method and basis dependence of the cross sections, reaction probabilities, scattering angle distributions, and so on. We carried out this unprecedented study for the $F^- + CH_3I$ reaction, reporting 20 different analytical PESs using the HF, MP2, MP2-F12, CCSD, CCSD-F12b, CCSD(T), CCSD(T)-F12b, and OQVCCD(T) ab initio methods and the B97-1, PBE0, M06-2X, and B2PLYP DFT functionals. For the HF and DFT methods the influence of dispersion corrections is also investigated, and basis set effects are studied using both the aug-cc-pVDZ and aug-cc-pVTZ bases for the HF, MP2, and MP2-F12 methods. The new analytical PESs allow computing millions of trajectories, resulting in statistically accurate scattering angle and internal energy distributions that can be directly compared with experiments.

The most important findings of the present study can be summarized as follows:

(a) A TZ basis provides smaller S_N2 inversion cross sections by about 20−30% relative to the HF and MP2 DZ results.
(b) The explicitly correlated F12 methods give similar TZ-quality cross sections with DZ and TZ basis sets.
(c) The quasi-variational OQVCCD(T) and CCSD(T) methods provide almost the same cross sections, showing that the PES, at least the selected configurations, can be well described by single-reference methods.
(d) The dynamics on the CCSD(T)-F12b/TZ-quality OSC PES (ref 8) and on the CCSD(T)-F12b/DZ PES are very similar.
(e) The four DFT functionals investigated in the present study all provide substantially larger S_N2 cross sections than the ab initio methods.
(f) For the retention S_N2 pathways the dependence of the cross sections on the electronic structure methods and, especially, basis sets is more significant than in the case of inversion. It seems that a TZ basis or an explicitly correlated method is needed to obtain substantial double-inversion reactivity.
(g) The HF method provides unreasonably large cross sections and qualitatively wrong, decaying excitation functions for the proton-transfer channel.
(h) The proton-transfer cross sections have significant basis set dependence, as a TZ basis provides twice as large reactivity compared with the DZ result.
(i) At a high collision energy most DFT functionals show significant reactivity at large impact parameters, resulting in slight dominance of forward scattering, whereas the ab initio methods give backward scattering, in agreement with experiment.
(j) The HF method provides too hot CH_3F internal energy distributions, shifted by ∼20 kcal/mol, in accord with the overestimated exothermicity.
(k) At low collision energies all ab initio correlation methods and DFT functionals give good agreement with the measured internal energy distributions. At high E_{coll}, the broad distributions are well reproduced, although the ab initio correlation methods slightly underestimate, whereas DFT overestimates the internal energy.

The present study shows that some details of the dynamics of the $F^- + CH_3I$ reaction can significantly depend on the level of electronic structure theory, whereas certain results seem to be converged with respect to the level of electron correlation and the size of the basis set. Considering the possible improvements of the theoretical description of the title reaction, two points should be mentioned besides the choice of the level of electronic structure theory, which is thoroughly investigated in the present study. First, the reaction dynamics simulations do not consider quantum effects, except the quasi-classical initial conditions. This may not be the reason for the experimental−theoretical discrepancies because at low E_{coll}, where the quantum effects are expected to be more significant, theory agrees well with experiment. Second, in the present study all of the PESs are developed based on the same set of geometries. In the future one may investigate the effect of the selection of the configurations on the dynamics because the accuracy of a fitted PES depends sensitively on the choice of the geometries. Thus one may further optimize the selection of the structures to obtain a better fit of the global PES, which may provide improved dynamics. We hope that the present study will help to close the gap between theory and experiment for the title reaction. Furthermore, the new results could be useful for any reaction dynamics simulation because the level of the electronic structure theory obviously affects the accuracy of the dynamics of a chemical system and the present study provides unprecedented insights into these effects.

■ ASSOCIATED CONTENT

Supporting Information

The Supporting Information is available free of charge on the ACS Publications website at DOI: 10.1021/acs.jpca.8b00770.

Numerical data for the cross sections, product channel branching ratios, reaction probabilities, scattering angle distributions, and product internal energy distributions corresponding to Figures 3−7, respectively. (PDF)

■ AUTHOR INFORMATION

Corresponding Author

*E-mail: gczako@chem.u-szeged.hu.

ORCID

Gábor Paragi: 0000-0001-5408-1748
Gábor Czakó: 0000-0001-5136-4777

Notes

The authors declare no competing financial interest.

DOI: 10.1021/acs.jpca.8b00770
J. Phys. Chem. A 2018, 122, 3353−3364

■ ACKNOWLEDGMENTS

G.C. thanks the National Research, Development and Innovation Office − NKFIH, K-125317 for financial support. We acknowledge the National Information Infrastructure Development Institute for awarding us access to resource based in Hungary at Szeged and Debrecen.

■ REFERENCES

(1) Born, M.; Oppenheimer, R. Zur Quantentheorie der Molekeln. *Ann. Phys.* **1927**, *389*, 457−484.
(2) Zhang, J.; Hase, W. L. Electronic Structure Theory Study of the $F^- + CH_3I \rightarrow FCH_3 + I^-$ Potential Energy Surface. *J. Phys. Chem. A* **2010**, *114*, 9635−9643.
(3) Zhang, J.; Mikosch, J.; Trippel, S.; Otto, R.; Weidemüller, M.; Wester, R.; Hase, W. L. $F^- + CH_3I \rightarrow FCH_3 + I^-$ Reaction Dynamics. Nontraditonal Atomistic Mechanisms and Formation of a Hydrogen-Bonded Complex. *J. Phys. Chem. Lett.* **2010**, *1*, 2747−2752.
(4) Mikosch, J.; Zhang, J.; Trippel, S.; Eichhorn, C.; Otto, R.; Sun, R.; de Jong, W. A.; Weidemüller, M.; Hase, W. L.; Wester, R. Indirect Dynamics in a Highly Exoergic Substitution Reaction. *J. Am. Chem. Soc.* **2013**, *135*, 4250−4259.
(5) Sun, R.; Davda, C. J.; Zhang, J.; Hase, W. L. Comparison of Direct Dynamics Simulations with Different Electronic Structure Methods. $F^- + CH_3I$ with MP2 and DFT/B97-1. *Phys. Chem. Chem. Phys.* **2015**, *17*, 2589−2597.
(6) Xie, J.; Zhang, J.; Hase, W. L. Is There Hydrogen Bonding for Gas Phase S_N2 Pre-Reaction Complexes? *Int. J. Mass Spectrom.* **2015**, *378*, 14−19.
(7) Zhang, J.; Xie, J.; Hase, W. L. Dynamics of the $F^- + CH_3I \rightarrow HF + CH_2I^-$ Proton Transfer Reaction. *J. Phys. Chem. A* **2015**, *119*, 12517−12525.
(8) Olasz, B.; Szabó, I.; Czakó, G. High-Level ab Initio Potential Energy Surface and Dynamics of the $F^- + CH_3I$ S_N2 and Proton-Transfer Reactions. *Chem. Sci.* **2017**, *8*, 3164−3170.
(9) Szabó, I.; Olasz, B.; Czakó, G. Deciphering Front-Side Complex Formation in S_N2 Reactions via Dynamics Mapping. *J. Phys. Chem. Lett.* **2017**, *8*, 2917−2923.
(10) Ma, Y.-T.; Ma, X.; Li, A.; Guo, H.; Yang, L.; Zhang, J.; Hase, W. L. Potential Energy Surface Stationary Points and Dynamics of the $F^- + CH_3I$ Double Inversion Mechanism. *Phys. Chem. Chem. Phys.* **2017**, *19*, 20127−20136.
(11) Liu, P.; Zhang, J.; Wang, D. Y. Multi-Level Quantum Mechanics Theories and Molecular Mechanics Study of the Double-Inversion Mechanism of the $F^- + CH_3I$ Reaction in Aqueous Solution. *Phys. Chem. Chem. Phys.* **2017**, *19*, 14358−14365.
(12) Ma, X.; Tan, X.; Hase, W. L. Effects of Vibrational and Rotational Energies on the Lifetime of the Pre-Reaction Complex for the $F^- + CH_3I$ S_N2 Reaction. *Int. J. Mass Spectrom.* **2017**, DOI: 10.1016/j.ijms.2017.07.011.
(13) Stei, M.; Carrascosa, E.; Kainz, M. A.; Kelkar, A. H.; Meyer, J.; Szabó, I.; Czakó, G.; Wester, R. Influence of the Leaving Group on the Dynamics of a Gas-Phase S_N2 Reaction. *Nat. Chem.* **2016**, *8*, 151−156.
(14) Czakó, G.; Bowman, J. M. Reaction Dynamics of Methane with F, O, Cl, and Br on ab Initio Potential Energy Surfaces. *J. Phys. Chem. A* **2014**, *118*, 2839−2864.
(15) Szabó, I.; Czakó, G. Dynamics and Novel Mechanisms of S_N2 Reactions on ab Initio Analytical Potential Energy Surfaces. *J. Phys. Chem. A* **2017**, *121*, 9005−9019.
(16) Hehre, W. J.; Radom, L.; Schleyer, P. v. R.; Pople, J. A. *Molecular Orbital Theory*; Wiley: New York, 1986.
(17) Møller, C.; Plesset, M. S. Note on an Approximation Treatment for Many-Electron Systems. *Phys. Rev.* **1934**, *46*, 618−622.
(18) Werner, H.-J.; Adler, T. B.; Manby, F. R. General Orbital Invariant MP2-F12 Theory. *J. Chem. Phys.* **2007**, *126*, 164102.
(19) Purvis, G. D., III; Bartlett, R. J. A Full Coupled-Cluster Singles and Doubles Model: The Inclusion of Disconnected Triples. *J. Chem. Phys.* **1982**, *76*, 1910−1918.
(20) Adler, T. B.; Knizia, G.; Werner, H.-J. A Simple and Efficient CCSD(T)-F12 Approximation. *J. Chem. Phys.* **2007**, *127*, 221106.
(21) Raghavachari, K.; Trucks, G. W.; Pople, J. A.; Head-Gordon, M. A Fifth-Order Perturbation Comparison of Electron Correlation Theories. *Chem. Phys. Lett.* **1989**, *157*, 479−483.
(22) Robinson, J. B.; Knowles, P. J. Breaking Multiple Covalent Bonds with Hartree−Fock-Based Quantum Chemistry: Quasi-Variational Coupled Cluster Theory with Perturbative Treatment of Triple Excitations. *Phys. Chem. Chem. Phys.* **2012**, *14*, 6729−6732.
(23) Hamprecht, F. A.; Cohen, A. J.; Tozer, D. J.; Handy, N. C. Development and Assessment of New Exchange-Correlation Functionals. *J. Chem. Phys.* **1998**, *109*, 6264−6271.
(24) Adamo, C.; Barone, V. Toward Reliable Density Functional Methods Without Adjustable Parameters: The PBE0Model. *J. Chem. Phys.* **1999**, *110*, 6158−6170.
(25) Zhao, Y.; Truhlar, D. G. The M06 Suite of Density Functionals for Main Group Thermochemistry, Thermochemical Kinetics, Noncovalent Interactions, Excited States, and Transition Elements: Two New Functionals and Systematic Testing of Four M06-Class Functionals and 12 Other Functionals. *Theor. Chem. Acc.* **2008**, *120*, 215−241.
(26) Grimme, S. Semiempirical Hybrid Density Functional with Perturbative Second-Order Correlation. *J. Chem. Phys.* **2006**, *124*, 034108.
(27) Grimme, S.; Antony, J.; Ehrlich, S.; Krieg, H. A Consistent and Accurate ab Initio Parametrization of Density Functional Dispersion Correction (DFT-D) for the 94 Elements H-Pu. *J. Chem. Phys.* **2010**, *132*, 154104.
(28) Grimme, S.; Ehrlich, S.; Goerigk, L. Effect of the Damping Function in Dispersion Corrected Density Functional Theory. *J. Comput. Chem.* **2011**, *32*, 1456−1465.
(29) Dunning, T. H., Jr. Gaussian Basis Sets for Use in Correlated Molecular Calculations. I. The Atoms Boron Through Neon and Hydrogen. *J. Chem. Phys.* **1989**, *90*, 1007−1023.
(30) Peterson, K. A.; Figgen, D.; Goll, E.; Stoll, H.; Dolg, M. Systematically Convergent Basis Sets with Relativistic Pseudopotentials. II. Small-Core Pseudopotentials and Correlation Consistent Basis Sets for the Post-*d* Group 16−18 Elements. *J. Chem. Phys.* **2003**, *119*, 11113−11123.
(31) Werner, H.-J.; Knowles, P. J.; Knizia, G.; Manby, F. R.; Schütz, M.; et al. *Molpro, version 2015.1, a package of ab initio programs*, see http://www.molpro.net.
(32) Braams, B. J.; Bowman, J. M. Permutationally Invariant Potential Energy Surfaces in High Dimensionality. *Int. Rev. Phys. Chem.* **2009**, *28*, 577−606.
(33) Bowman, J. M.; Czakó, G.; Fu, B. High-Dimensional ab Initio Potential Energy Surfaces for Reaction Dynamics Calculations. *Phys. Chem. Chem. Phys.* **2011**, *13*, 8094−8111.
(34) Hase, W. L. *Encyclopedia of Computational Chemistry*; Wiley: New York, 1998; pp 399−407.
(35) Szabó, I.; Czakó, G. Revealing a Double-Inversion Mechanism for the $F^- + CH_3Cl$ S_N2 Reaction. *Nat. Commun.* **2015**, *6*, 5972.
(36) Paul, A. K.; Hase, W. L. Zero-Point Energy Constraint for Unimolecular Dissociation Reactions. Giving Trajectories Multiple Chances to Dissociate Correctly. *J. Phys. Chem. A* **2016**, *120*, 372−378.

DOI: 10.1021/acs.jpca.8b00770
J. Phys. Chem. A 2018, 122, 3353−3364